# VACT: Visualization-Aware CT Reconstruction

Ziyi Zheng and Klaus Mueller, *Senior Member, IEEE*

Visual Analytics and Imaging Lab, Computer Science Department
Stony Brook University, NY and SUNY Korea

***Abstract*— Computed tomography (CT) reconstruction methods are often unaware of the requirements of the subsequent 3D volume visualization stage. In this stage, a delicate and often-studied component is the interpolation of off-grid samples, where aliasing can lead to misleading artifacts and blurring, potentially hiding fine details of critical importance. The visualization-aware CT reconstruction framework we describe aims to account for these errors directly in the volume generation stage. Our framework informs the CT reconstruction process of the specific filter intended for interpolation in the subsequent visualization process, and this in turn ensures an accurate interpolation there at a set tolerance. Here, we focus on fast trilinear interpolation in conjunction with an octree-type mixed resolution volume representation without T-junctions. Efficient rendering is achieved by a space-efficient and locality-optimized representation, which can straightforwardly exploit fast fixed-function pipelines on GPUs.**

## I. Introduction

Medical routine frequently utilizes 3D visualization tools for diagnosis. Computed tomography (CT) acquires X-ray projection data of an object or patient from different vantage points and subsequently employs CT reconstruction to produce these volume data sets. Via direct volume rendering (DVR), users can then look for fine details such as hairline fractures, small pathological features such as tumors, and textures of diagnostic value. To be useful, the volume visualization tools must form a reliable basis for their judgment. Additionally, users also require interactive rendering speed to freely examine the data.

Much research has focused on recovering fine details from volumetric data by designing and using interpolation filters of higher quality. These filters are mostly based on theoretical derivations and do not consider the origin of the data, in our case CT reconstruction, themselves. However, as is the case for CT, the volumetric data subject to interpolation in the rendering stage are not the actual raw data, but only derived from them. Thus, any quality-enhancing effort neglecting this transformation stage cannot guarantee verifiable results. Therefore visualization-aware CT reconstruction pipeline must integrate the rendering stages with the scalar field generation.

In order to address these shortcomings into practice, we propose a framework we call visualization-aware CT, or VACT. Our procedure bridges the currently existing disconnect between the raw projection data and their visualization via volume rendering. Our framework can guarantee a pre-set error tolerance that is applied in the CT reconstruction step. The VACT framework is related to our VDVR system that addresses these problems from a visualization perspective [1].

Email: {zizhen, mueller}@cs.sunysb.edu).

## II. Approach

Our pipeline is shown in Fig. 1. The inputs are the X-ray projections and an error threshold ε. We first determine the upsampling rate of the filtered projections by estimating the error bound. This analysis is based on the projections after ramp-filtering. Then we run frequency domain upsampling according to the verified upsampling rate and ramp-filter the upsampled projections. Following, we perform a CT reconstruction at the Nyquist resolution (1× up-sampling), perform the error analysis and determine the ε-verified oversampling rate for the 3D volume. Then we perform back-projection again but now on a high-resolution grid which captures all possible details. We call this the gold-standard. To keep within the memory limit, we generate the gold standard in blocks of multiple cells. Within each such block, and from the gold-standard, we then build a mixed-resolution representation only keeping the detail needed. Starting from the typical base resolution commonly used, we classify those cells as subdivision cells which contain finer details. These cells are then represented with more data points. Finally, any potential T-junctions in the mixed-resolution data are removed.

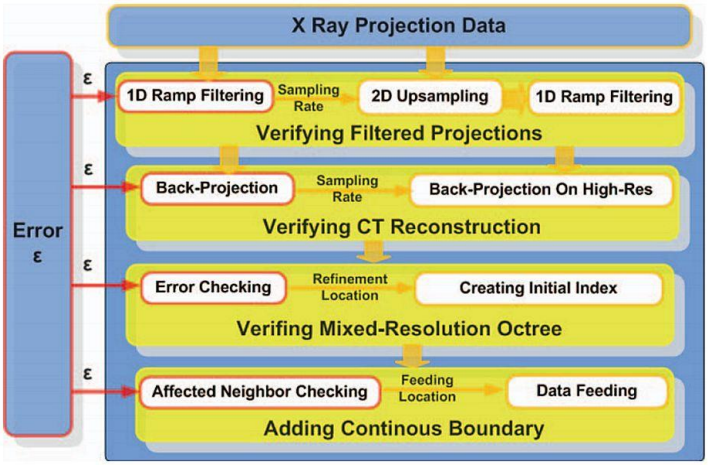


Fig. 1. The visualization-aware CT reconstrruction pipeline

Let us now investigate the reconstruction for a linear interpolation filter – the trilinear filter is an extension of this derivation. For the linear filter the largest error occurs at the local peak or valley where the maximum curvature is located [2]. Fig. 2 illustrates this scenario for a single frequency, where the largest error occurs around the sine function's peak. Given the

sampling distance $d$, the max absolute error $E_j$ for a specific wavelength with amplitude $A_i$ is:

$$E_i = |A_i|(1-\sin(\frac{2\pi}{T_i}(\frac{1}{4}T_i - \frac{d}{2}))) \quad d < T_i/2 \qquad (1)$$

where the maximum interpolation error $E_i$ is a function of the sampling distance $d$ and the signal period $T_i$. The distance $d$ and period $T_i$ are connected by the oversampling rate. If $d=T_i/2$, the sampling rate is just below the Nyquist sampling rate. In this case, the maximum error for linear interpolation could be 100% of the sine peak value. If $d=T_i/16$ (equivalent to an 8× oversampling rate), this will guarantee that the error is less than 1.92% of the maximum (peak) value. Fig. 2b illustrates the error as a function of oversampling rate and signal frequency. The error decreases with increasing oversampling rate and/or decreasing signal frequency.

Of course, a signal is a composite of multiple frequencies and therefore these errors would possibly compound. However, most likely these frequencies would be phase shifted which would reduce the local curvature and thus alleviate the error.

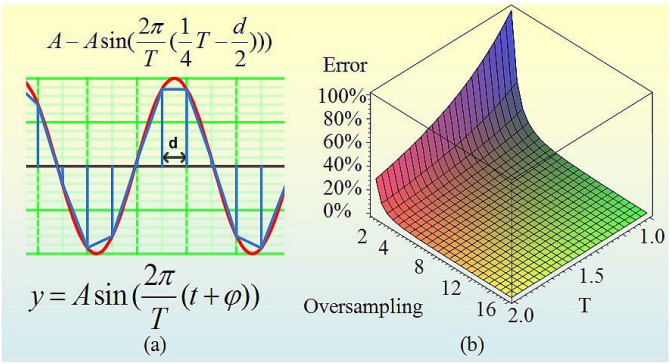


Fig. 2. *Sine* signal reconstructed with linear interpolation and error.

## III. Results

Fig. 3 shows volume renderings of a carp dataset, where 142 projections of resolution 256×129 each were used for reconstruction to obtain both the traditional volume dataset pictured on the top and the VACT representation pictured at the bottom. Using these simulated projections the dataset was reconstructed and then rendered using a standard trilinear interpolation filter. Fig. 3 panels (a), (d) and (f), were rendered from a uniform $128^2$×256 volume (base) resolution, which is the resolution one would typically pick given the 256×129 projection data. We observe strong aliasing artifacts in these renderings. On the other hand, the renderings obtained from the mixed-resolution volume (3% error threshold, 2.4× more storage) and shown in panels (c), (e) and (h) can resolve small detail, such as the thin bones, rather well. We also took the base resolution volume of (d) and used frequency domain upsampling to generate a volume of the same storage than the mixed resolution of (e). Panels (b) and (g) show magnified cuts of a rendering of this volume.

## IV. Conclusions

We presented a framework that informs the CT reconstruction pipeline by the possible errors committed in a subsequent 3D volume visualization procedure. While we have demonstrated our pipeline not with a human medical CT dataset, similar observations apply. Future work will also adapt these concepts for more efficient grids, such as BCC [3][4], and we also plan to evaluate and incorporate other errors occurring in the rendering such as shading, gradient estimation, transfer functions, perception, and the like.

*Acknowledgements:* Partial funding was provided by NSF grant IIS 1117132.

## References

[1] Z. Zheng, W. Xu, K. Mueller, "VDVR: Verifiable Volume Visualization of Projection-Based Data," *IEEE Transactions on Visualization and Computer Graphics*, 16(6):1515-1524, 2010.

[2] J. Smith, P. Gossett. "A Flexible Sampling-Rate Conversion Method," Proc. IEEE Int'l Conf. Acoustics, Speech, & Signal Proc, pp. 112-115, 1984. (Tutorial at http://ccrma.stanford.edu/~jos/resample)..

[3] J. Conway and N. Sloane. *Sphere Packings, Lattices and Groups*. Springer, 3rd edition, 1999.

[4] F. Xu and K. Mueller, "Optimal Sampling Lattices for High-Fidelity CT Reconstruction," *IEEE Medical Imaging Comf.*, Orlando, October, 2009

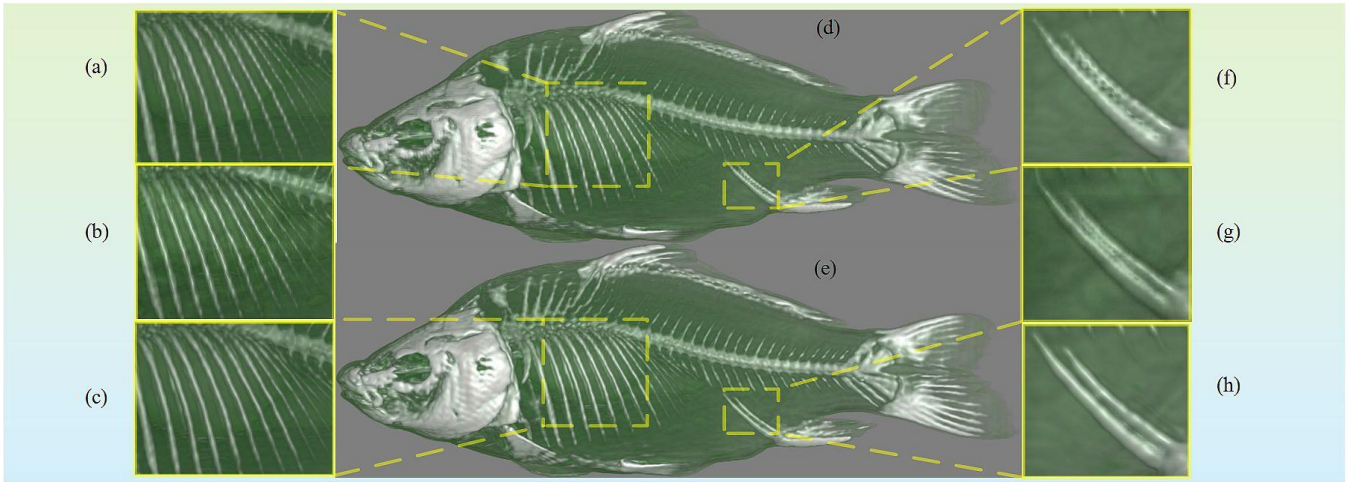


Fig. 3. Renderings of a carp dataset represented in the various grid resolution types. (a)(d)(f) uniform (coarse) resolution, (c)(e)(h) mixed-resolution, (b)(d) frequency-domain upsampled resolution using the same storage than the mixed resolution (magnified cuts only).